electronics

Article

Influence Analysis of Voltage Imbalance in Input-Series, Output-Parallel (ISOP) Multichannel IPT System

Leyu Wang, Pan Sun *, Yan Liang, Xusheng Wu and Enguo Rong

School of Electrical Engineering, Naval University of Engineering, Wuhan 430033, China; m22380811@nue.edu.cn (L.W.); 20100502@nue.edu.cn (Y.L.); 0910061003@nue.edu.cn (X.W.); 21100506@nue.edu.cn (E.R.)

* Correspondence: 1007101026@nue.edu.cn

Abstract: In order to solve the demand for efficient and stable low-voltage, high-power energy transmission capacity of electric vehicle (EV) fast charging, an ISOP-IPT system based on inductor-capacitor-capacitor series (LCC-S) compensation network is proposed. Firstly, the influence of compensation parameter inconsistency on the system is analyzed. On this basis, considering the resistance of coupler coils, the overall transmission efficiency of the system is analyzed. It is found that the voltage imbalance of the system will affect the working state of inverters, and then affect the stability of the system. The system transmission efficiency increases with the increase in mutual inductance. Moreover, the voltage imbalance caused by the inconsistency of compensation parameters and mutual inductance will reduce the transmission efficiency of the system. Finally, it is concluded that in the parameter design of the ISOP-IPT system, mutual inductance should be improved on the basis of ensuring the input voltage equalization of each channel so as to improve the transmission efficiency and working stability of the system. The experimental platform of a two-channel ISOP-IPT system is built and the maximum efficiency is 94.03%, which verifies the correctness of theoretical analysis.

Keywords: input-series; output-parallel; inductive power transfer; transmission efficiency; voltage imbalance

Citation: Wang, L.; Sun, P.; Liang, Y.; Wu, X.; Rong, E. Influence Analysis of Voltage Imbalance in Input-Series, Output-Parallel (ISOP) Multichannel IPT System. *Electronics* **2024**, *13*, 1865. https://doi.org/10.3390/electronics13101865

Academic Editor: Fabio Corti

Received: 9 April 2024
Revised: 3 May 2024
Accepted: 8 May 2024
Published: 10 May 2024

1. Introduction

Compared to traditional wired charging methods, inductive power transfer (IPT) technology achieves physical electrical isolation through couplers, thus offering higher safety, flexibility, and convenience, making it a hot research topic [1,2]. IPT technology has been widely used in various fields, such as electric vehicles (EVs) [3,4], implantable medical treatment [5], underwater vehicles [6,7], mobile electronic equipment [8], and so on. At the same time, because the process of connecting the charging line is eliminated, the automatic charging of unmanned devices also provides favorable realization conditions [9].

At present, the promotion of EVs is mainly affected by the problem of driving range. Due to the limitation of battery materials, it is difficult to achieve significant improvement in battery capacity. Therefore, it is necessary to study the problem of low-voltage and high-power demand for fast charging of EVs. In order to improve the transmission power of an IPT system, many scholars have made contributions in related fields and proposed circuit structures such as multi-inverter parallel [10], multi-transmit channel parallel [11], multi-inverter multi-rectifier [12], and so on. In Ref. [10], a multi-inverter parallel structure based on a resonant inductor integrated transformer is proposed, which effectively improves the transmission power on the transmitting side. In Ref. [11], an input parallel structure based on a single switching circuit is proposed, which improves power while reducing switching loss compared with traditional inverters. In Ref. [12], a DC parallel AC series structure with multi-inverter multi-rectifier is proposed to realize power sharing among multiple converters. The circuit structure in the above study not only increases the transmission power of the IPT system but also significantly increases the DC bus current on the transmitting side and increases the current loss of the system. In addition, when using a single coupling coil for high-power energy transmission in the AC part, it will also challenge the heat dissipation capacity of the system, which is not conducive to long-term continuous demands.

For the input-series, output-parallel (ISOP) multichannel IPT system, the power transmission capacity of the system can be improved by increasing the input voltage level while keeping the current of the DC bus unchanged. The system transmission power is distributed to each channel, reducing the rated power demand of a single-channel device, thereby reducing the system cost and heat dissipation pressure. Some scholars have analyzed the IPT system with ISOP circuit structure [13,14]. In Ref. [13], a closed-loop control strategy of input voltage equalization and output constant voltage (CV) for an ISOP-IPT system was proposed. However, the paper did not provide an analysis of transmission characteristics when the system voltage is imbalanced. In Ref. [14], a hybrid IPT topology is proposed and the ISOP structure on the AC side is analyzed. The tolerance of coil misalignment in the IPT system is improved. However, the above studies are aimed at improving the stability of the IPT system. The characteristics of an ISOP multichannel IPT system have not been analyzed.

During the design process of an ISOP-IPT system, component parameters are affected by factors such as manufacturing error or element aging, which inevitably cause parameter deviation. The equivalent input impedance of each channel will change with the change in compensation element parameters, mutual inductance, and load resistance. Because the DC input side of the multichannel system adopts a series circuit structure, the equivalent input impedance of each channel will directly affect the distribution of the input voltage. There are relatively few studies on the influence of parameter inconsistency in multichannel ISOP-IPT systems. Therefore, in this paper, the influence of parameter offset and voltage imbalance of an ISOP-IPT system based on an inductor–capacitor–capacitor series (LCC-S) compensation network is analyzed, and the theoretical equation of the overall transmission efficiency of the system is given. Theoretical support for the parameter design of the ISOP-IPT system is provided.

The structure of this paper is as follows. In Section 2, the influence of parameter deviation of the ISOP-IPT system on input voltage balancing state is analyzed. In Section 3, the influence of voltage imbalance on the transmission efficiency of the ISOP-IPT system is analyzed. In Section 4, the correctness of the theoretical analysis is verified by experiments. Finally, Section 5 concludes this paper.

2. Influence Analysis of Parameter Offset on Input Voltage Equalization State in ISOP Multichannel IPT System

For the IPT system, four basic compensation networks (S-S, S-P, P-S, P-P), have the advantages of simple structure and low cost [15]. However, because the circuit structure is relatively simple, the system is sensitive to the change in compensation parameters. When the ZVS working state of the inverter is adjusted, the compensation parameter will deviate from the resonant point and affect the transmission efficiency of the system. In order to improve the design freedom of the system, a high-order compensation network is proposed and studied. LCC-S and double-sided LCC (DLCC) compensation networks have received more attention and research due to the constant current characteristics of transmitting coil branches independent of load and mutual inductance [16,17]. However, because the receiving side of the DLCC compensation network contains compensating inductors, the receiving-side volume will increase in the case of multichannel operation, which is not conducive to the lightweight design of the system. Therefore, an LCC-S compensation network is more suitable for an ISOP multichannel IPT system.

Considering that the parameter offset of the system compensation element will inevitably occur in the process of machining and installation, its influence is analyzed. Figure 1 shows the basic circuit structure of the ISOP multichannel IPT system. U_{in} and I_{in} are the DC input voltage and current. The system realizes current conversion through full-bridge inverters (G_1–G_4) and rectifiers (D_1–D_4). L_{pi} and L_{si} are the coupling coils' self-inductance. $M_{\rm i}$ is the mutual inductance of each channel. $C_{{\rm in}i}$ and $C_{{\rm o}i}$ are DC filter capacitors. $R_{\rm L}$ is the load resistance.

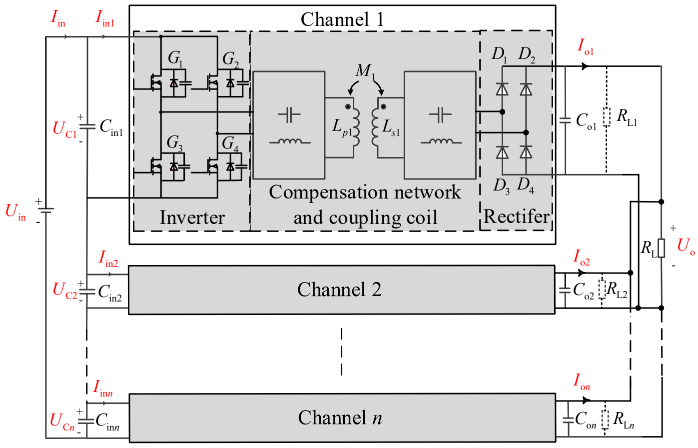

Figure 1. Multi-channel ISOP-IPT system circuit structure diagram.

The ISOP-IPT system satisfies the circuit structure relation in Equation (1):

$$\begin{cases} I_{{\rm in}i} = I_{{\rm in}j} \\ U_{{\rm Co}i} = U_{{\rm Co}j} \\ U_{\rm in} = \sum\limits_{i=1}^{n} U_{{\rm C}i} \\ I_{\rm o} = \sum\limits_{i=1}^{n} I_{{\rm o}i} \end{cases} \tag{1}$$

where $I_{{\rm in}i}$ and $I_{{\rm o}i}$ are the input and output currents of each channel. $U_{{\rm C}i}$ and $U_{{\rm Co}i}$ are the input and output voltages of each channel.

Combined with Equation (1) and the voltage conservation law, it can be concluded that the proportional relationship between voltage and current of each channel in the ISOP-IPT system is:

$$\frac{U_{{\rm C}i}}{U_{{\rm C}j}} = \frac{I_{{\rm o}i}}{I_{{\rm o}j}} = \frac{L_i M_j}{L_j M_i} = \frac{R_{{\rm eq}j}}{R_{{\rm eq}i}} \tag{2}$$

In order to improve the transmission efficiency of the IPT system, the condition of full resonance is usually satisfied when the parameters of the compensation network are designed. On this basis, the offset coefficients $k_{{\rm L}i}$, $k_{{\rm C}i}$, $k_{{\rm Cp}i}$ and $k_{{\rm Cs}i}$ of component parameters are added to analyze the influence of component parameter offset on the system.

Figure 2 shows the equivalent circuit diagram of each channel based on the LCC-S compensation network, where L_i, C_i and $C_{{\rm p}i}$ constitute the transmitting side compensation network and C_{si} is the receiving side compensation capacitor. The self-inductance and transmission mutual inductance of the coupling coils are $L_{{\rm p}i}$, $L_{{\rm s}i}$ and M_i, respectively.

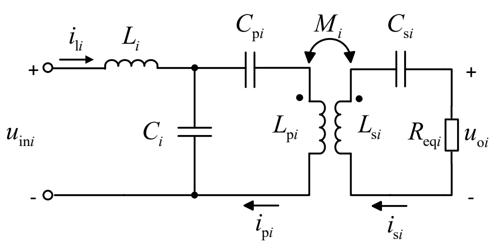

Figure 2. Equivalent circuit diagram of each channel based on LCC-S compensation network.

According to the equivalent circuit of the LCC-S compensation network shown in Figure 2, the steady-state circuit equation of each channel can be obtained based on Kirchhoff's law:

$$\begin{cases} j\omega k_{\mathrm{L}i}L_i\dot{I}_{\mathrm{l}i} + \frac{1}{j\omega k_{\mathrm{C}i}C_i}(\dot{I}_{\mathrm{l}i} - \dot{I}_{\mathrm{p}i}) = \dot{U}_{\mathrm{in}i} \\ \frac{1}{j\omega k_{\mathrm{C}i}C_i}(\dot{I}_{\mathrm{p}i} - \dot{I}_{\mathrm{l}i}) + (\frac{1}{j\omega k_{\mathrm{Cp}i}C_{\mathrm{p}i}} + j\omega L_{\mathrm{p}i})\dot{I}_{\mathrm{p}i} - j\omega M_i\dot{I}_{\mathrm{s}i} = 0 \\ (\frac{1}{j\omega k_{\mathrm{Cs}i}C_{\mathrm{s}i}} + j\omega L_{\mathrm{s}i} + R_{\mathrm{eq}i})\dot{I}_{\mathrm{s}i} - j\omega M_i\dot{I}_{\mathrm{p}i} = 0 \end{cases} \tag{3}$$

By simplifying Equation (3), the receiving circuit impedance of each channel can be obtained under the condition of non-resonance when the influence of migration is considered:

$$Z_{\mathrm{s}i} = \frac{1}{j\omega k_{\mathrm{Cs}i}C_{\mathrm{s}i}} + j\omega L_{\mathrm{s}i} + R_{\mathrm{eq}i} \tag{4}$$

The RMS value of rectifier input voltage for each channel is calculated as:

$$\begin{cases} U_{\mathrm{o}i} = \left|\dot{I}_{\mathrm{o}i}\right|R_{\mathrm{eq}i} = \frac{|j\omega M_i Z_{\mathrm{Y}i}|R_{\mathrm{eq}i}}{|Z_{\mathrm{s}i}Z_{\mathrm{X}i}|}U_{\mathrm{in}i} \\ Z_{\mathrm{X}i} = 1 - \omega^2 k_{\mathrm{C}i}C_i L_{\mathrm{p}i} + \frac{k_{\mathrm{C}i}C_i}{k_{\mathrm{Cp}i}C_{\mathrm{p}i}} + \frac{j\omega^3 M_i^2 k_{\mathrm{C}i}C_i}{Z_{\mathrm{s}i}} \\ Z_{\mathrm{Y}i} = \frac{j\omega k_{\mathrm{C}i}C_i}{1-\omega^2 k_{\mathrm{C}i}C_i k_{\mathrm{L}i}L_i - Z_{\mathrm{X}i}^{-1}} \end{cases} \tag{5}$$

By combining Equations (1), (2) and (5), the parameter proportional relationship of each channel in the ISOP-IPT system can be obtained:

$$\begin{cases} 1 = \frac{|Z_{\mathrm{s}i}Z_{\mathrm{X}i}|\left|j\omega M_j Z_{\mathrm{Y}j}\right|}{\left|Z_{\mathrm{s}j}Z_{\mathrm{X}j}\right||j\omega M_i Z_{\mathrm{Y}i}|} \\ \frac{1}{R_{\mathrm{L}}} = \sum\limits_{i=1}^{n}\frac{1}{R_{\mathrm{L}i}} \end{cases} \tag{6}$$

It can be seen from Equation (6) that for a multichannel system under non-resonant conditions, the relationship between the voltage ratio of each channel on the DC input side and the parameters of the compensation element satisfy a complex implicit function equation set, which is further complicated by the increase in the number of channels. Compensation network parameters, transmission mutual inductance and load resistance all affect voltage distribution. For multichannel ISOP-IPT systems, when the compensation network parameters are determined and the influence of cross-inductance is ignored, the AC circuits of each channel will not interact with each other, and can be equivalent to multiple single-channel systems for analysis. The change in the relationship between channels in the whole system is mainly reflected in the DC side. The minimum multichannel system with two channels can also reflect the characteristics of voltage proportional relationship. In order to simplify the analysis process, the two-channel ISOP-IPT system was simulated and analyzed, and the parameters of resonant compensation elements in each channel are shown in Table 1.

Table 1. Simulation parameters of 2-channel ISOP-IPT system.

Symbol	Value	Symbol	Value
$L_i/\mu\mathrm{H}$	15	C_i/nF	233.7
$L_{\mathrm{p}i}/\mu\mathrm{H}$	95	$C_{\mathrm{p}i}/\mathrm{nF}$	43.824
$L_{\mathrm{s}i}/\mu\mathrm{H}$	95	$C_{\mathrm{s}i}/\mathrm{nF}$	36.904
$M_i/\mu\mathrm{H}$	20	R_{L}/Ω	5
$U_{\mathrm{in}}/\mathrm{V}$	470	f/kHz	85

Based on the above parameters of resonant elements, the relationship curves between input voltage ratio $K_{\mathrm{U}ij}$ and transmission mutual inductance ratio k_{M} of each channel are analyzed under different offset coefficients. In addition, the mutual inductance ratio is increased from 0.5 to 1.5 during simulation analysis.

(a) Influence analysis of the inductance offset on transmitting side

As can be seen from Figure 3, when the L_1 deviates from the resonant condition, the relationship between input voltage ratio and transmission mutual inductance ratio is little affected, the input voltage imbalance of the system is mainly affected by the inconsistent transmission mutual inductance, and the two are inversely proportional.

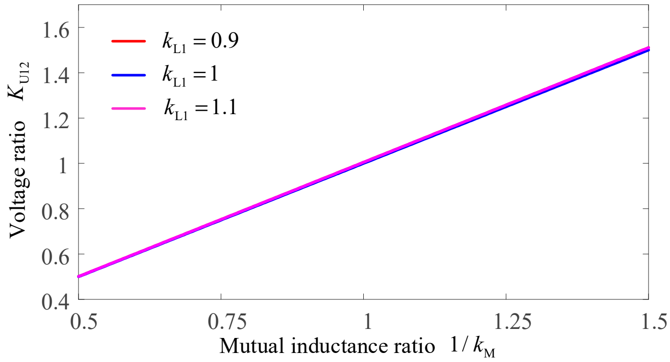

Figure 3. The relationship curve between K_{Uij} and k_M when the series compensation inductor L_1 of channel 1 is offset.

(b) Influence analysis of the compensating capacitance offset

Figure 4 shows the effect on the relationship between input voltage ratio and transmission mutual inductance ratio when the compensating capacitance of channel 1 deviates from the resonant point. It can be seen that when the C_{pi} is offset, it has little effect on the voltage imbalance of the system. However, when C_i and C_{si} are offset, the proportional coefficient between k_{Uij} and k_M will be changed, which will have a great impact on the voltage imbalance state of the system. When the M_i of the system is consistent, the offset of C_i and C_{si} will increase the voltage imbalance of the system.

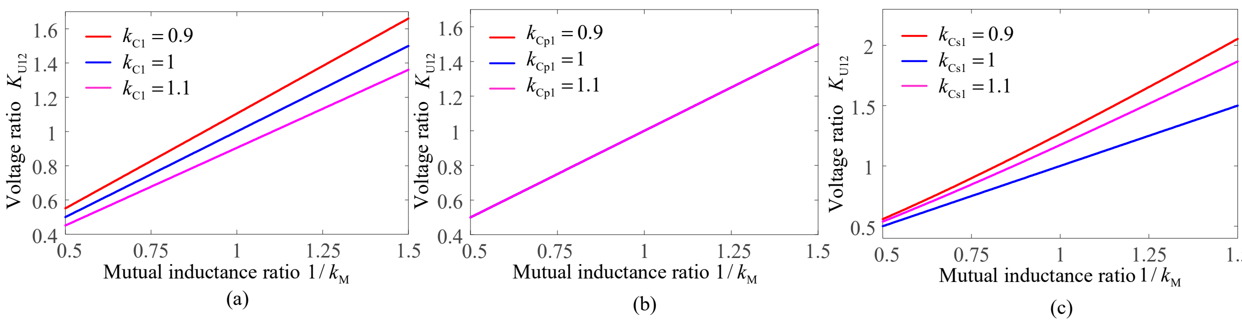

Figure 4. Curves of K_{Uij} and k_M when the compensating capacitance of channel 1 is offset. (**a**) C_1, (**b**) C_{p1}, (**c**) C_{s1}.

Under the condition that the mutual inductance of each channel is consistent, the influence of C_i and C_{si} on the input voltage equalization of the system is analyzed. Parameters of each channel component in Table 1 are still used for simulation, and the simulation results are shown in Figure 5.

According to the analysis in Figure 5, when the mutual inductance of all channels is consistent, the compensated network parameter offset will affect the input voltage equalization of the system. In Figure 5a, the offset coefficient of compensation capacitance on the receiving side of channel 2 is 1, and it can be seen that the overall relation surface shifts downward as k_{C2} decreases and upward as k_{C2} increases. The change in the input voltage ratio between channels is opposite to the offset of shunt compensation capacitance of channel 1, and the correlation between the two is proportional to the offset of compensation capacitance of channel 1. In Figure 5b, the offset coefficient of the parallel compensation capacitor of channel 2 is 1, and the relationship change curve is translated downward as a whole with the offset of the compensation capacitor at the receiving side of channel 2. At this time, the parameter offset of channel 1 and the input voltage ratio between channels maintain the same change relationship as shown in Figure 5a.

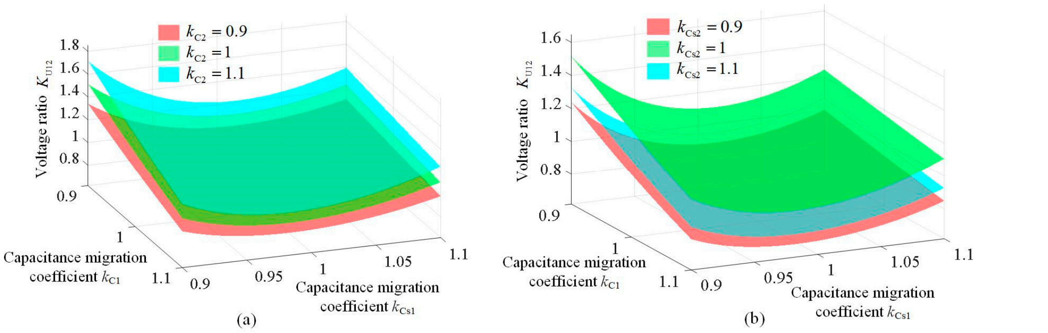

Figure 5. The influence of C_i and C_{si} simultaneous migration on the system input voltage equalization. (**a**) $k_{Cs2} = 1$, (**b**) $k_{C2} = 1$.

In general, when the mutual inductance of each channel is consistent, the shunt compensation capacitance offset on the transmitting side is inversely proportional to the partial voltage of the corresponding channel. At the same time, the greater the offset degree of the compensation capacitor on the receiving side, the greater the voltage input of the corresponding channel.

(c) Influence analysis of load resistance change

Take the wireless charging of EVs as an example. During the charging process, the load impedance of the DC output of the system will change. Make the channel parameters of the ISOP-IPT system consistent and meet the resonant conditions, as shown in Table 1. According to Equation (6), when the load impedance changes, the relationship among the system input voltage ratio, mutual inductance ratio, and parameter offset coefficient is analyzed. The simulation results are shown in Figure 6.

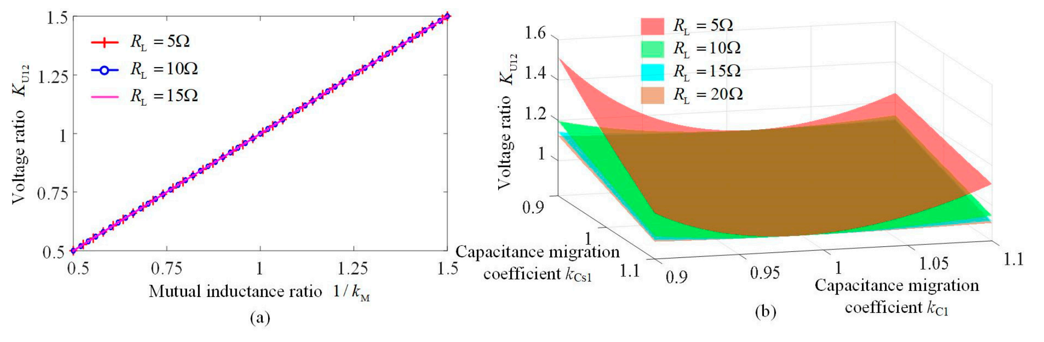

Figure 6. Curve of system input voltage ratio affected by mutual inductance ratio and parameter offset when load resistance changes. (**a**) $1/k_M$. (**b**) k_{C1}, k_{Cs1}.

According to the analysis of the simulation results in Figure 6a, when the parameters of each channel in the ISOP system are consistent and the resonant conditions are met, the ratio of input voltage is inversely proportional to the ratio of mutual inductance. As can be seen from Figure 6b, in the case of small load, the system transmission power is higher, and the ratio of input voltage is more affected by the parameter offset of C_i and C_{si}. With the increase in load resistance, the transmission power of the system decreases, and the influence of parameter offset of C_i and C_{si} also decreases obviously.

3. Influence Analysis of Voltage Imbalance in ISOP Multichannel IPT System Based on LCC-S Compensation Network

From the analysis in the previous section, it can be seen that the compensated network parameter offset of the ISOP-IPT system will cause the input voltage of the DC side to be imbalanced. Therefore, it is necessary to analyze the influence of imbalanced input voltage in the system.

3.1. Influence Analysis of Voltage Imbalance on the ZVS Working State of the System

According to Equation (1), the ISOP-IPT system is based on the DC side series and parallel circuit structure, which improves the system's ability to withstand input voltage and output current, thus improving the system's power transmission capability.

The compensation network of each channel in an ISOP-IPT system usually satisfies the condition of full resonance:

$$\omega^2 = \frac{1}{L_i C_i} = \frac{1}{C_{\mathrm{p}i}\left(L_{\mathrm{p}i} - L_i\right)} = \frac{1}{L_{\mathrm{s}i} C_{\mathrm{s}i}} \tag{7}$$

where w is the system resonance angular frequency.

In the case of resonance, the voltage relationship between the two ends of each channel inverters of the system is:

$$U_{\mathrm{in}i} = \frac{2\sqrt{2}}{\pi} U_{\mathrm{C}i} \sin\left(\frac{\theta}{2}\right) \tag{8}$$

where θ_i is the conduction angle of each channel inverter.

Based on Equation (7), the I_{pi} can be obtained:

$$I_{\mathrm{p}i} = \frac{U_{\mathrm{in}i}}{jX_{\mathrm{L}i}} = \frac{U_{\mathrm{in}i}}{j\omega L_i} \tag{9}$$

where $X_{\mathrm{L}i}$ is the inductive reactance of the series compensation inductance of each channel.

Equivalent impedance $R_{\mathrm{eq}i}$ on each channel rectifier input side is:

$$R_{\mathrm{eq}i} = \frac{8}{\pi^2} R_{\mathrm{L}i} = \frac{8U_{\mathrm{o}i}}{\pi^2 I_{\mathrm{o}i}} \tag{10}$$

From the above equation, the receiver side reflection impedance $Z_{\mathrm{rec}i}$ of the transmitting coil branch can be obtained:

$$Z_{\mathrm{rec}i} = \frac{(\omega M_i)^2}{R_{\mathrm{eq}i}} \tag{11}$$

Due to the filtering effect of the LC resonant loop in the transmitting side, the harmonic effect of the transmitting coil branch can be ignored, but the $I_{\mathrm{l}i}$ flowing through the L_i contains harmonic components. According to the analysis in [18], combined with the fundamental harmonic approximation method and harmonic model, the time-domain expression of the output current at the switching time of the inverter is obtained:

$$I_{\mathrm{l}i}(t_0) = -\frac{U_{\mathrm{C}i}\theta_i}{2X_{\mathrm{L}i}} + \frac{2U_{\mathrm{C}i}Z_{\mathrm{rec}i}}{\pi X_{\mathrm{L}i}^2}\sin(\theta_i) + \frac{2U_{\mathrm{C}i}}{\pi X_{\mathrm{L}i}}(1 - \cos(\theta_i)) \tag{12}$$

where θ_i is the conduction angle of the inverter in each channel.

In order to simplify the analysis process, it is assumed that the parameters of compensation network and mutual inductance of each channel in ISOP-IPT system are identical. Combined with Equation (12), when the DC input voltage of each channel is 300 V and the load resistance is 10 Ω, the output current value of the inverter at the switching time varies with θ_i, as shown in Figure 7. In an IPT system, in order to realize ZVS working state, the equivalent input impedance of the system is usually required to be weakly inductive, and the instantaneous current at the switching time of inverter is less than a certain value [19]. Taking 3A as the instantaneous current reference value, it can be seen that the ISOP-IPT system based on LCC-S compensation network can work in the ZVS state under the condition of full resonance without external control. Moreover, the instantaneous current value of the switching time decreases with the increase in the DC input voltage of each channel in the system.

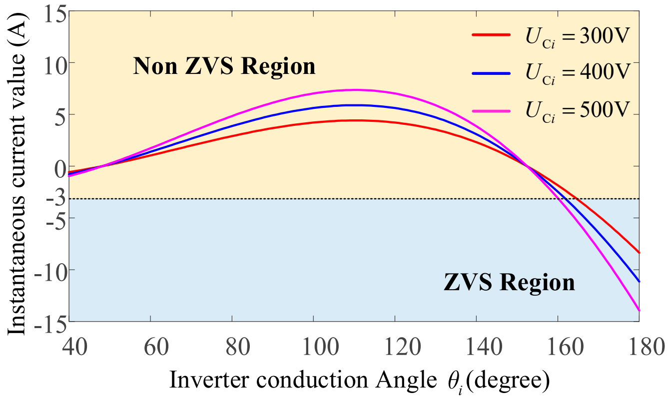

Figure 7. The curves of the instantaneous current value with θ_i at the switching time of the inverter.

Since the DC input side of the ISOP-IPT system is series, the voltage distribution of each channel will be affected by the equivalent impedance when the total input voltage is unchanged. The variation coefficient of DC input voltage of channel i is k_{Ui}, and the variation coefficient of the corresponding rectifier input equivalent impedance R_{eqi} is $1/k_{Ui}$. At this time, taking the two-channel system as an example, the instantaneous current value change at the switching time of the inverter in channel 1 is shown in Figure 8. The amplitude of $I_{11}(t_0)$ decreases with the decrease in the DC input voltage, and the equivalent input impedance of each channel has weak sensitivity. However, in the channel with lower transmission power, the inverter may lose the ZVS operating state due to the lower sensibility of the equivalent impedance.

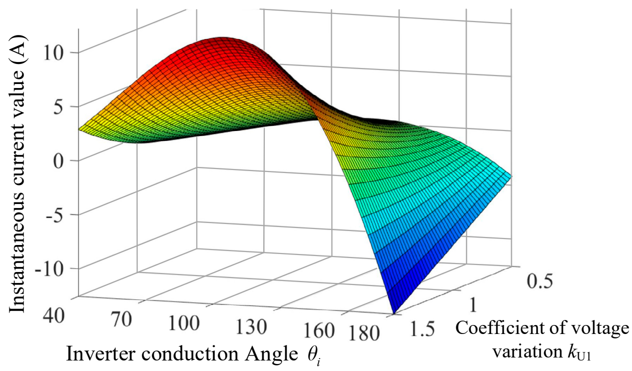

Figure 8. The instantaneous output current I_{11} (t_0) of the inverter with conduction angle θ_i and input voltage change.

Based on the above analysis, it can be seen that the increase in DC input voltage imbalance in the ISOP-IPT system will cause the channels with low partial voltage to gradually lose the ZVS working state. The inverter switching loss increases, affecting the stability of the system.

3.2. Influence Analysis of Voltage Imbalance on System Transmission Efficiency

The transmission efficiency equation of the ISOP multichannel IPT system is derived before analyzing the effect of input voltage imbalance on transmission efficiency. For a multichannel ISOP-IPT system, in order to improve the transmission efficiency of the system, it is usually necessary to make the inverters work in ZVS state by parameter design. Under the resonant condition, the mutual inductance and compensation parameters of each channel are consistent as much as possible so as to achieve the input voltage equalization on the DC side. On this basis, the transmission power loss of the system mainly comes from two sources: one is the resistance of the coupling coils, and the other is the converter loss.

The converter loss of a single channel can be divided into conduction loss and switching loss. The converter power loss formula is [20]:

$$\begin{cases} P_{\mathrm{c1}} = 2R_{\mathrm{DS}}I_{\mathrm{P}}^2 + \frac{\sqrt{2}U_{\mathrm{SD}}I_{\mathrm{P}}}{\pi}\left[2 - 2\cos\left(\frac{\alpha}{2}\right)\right] \\ P_{\mathrm{c2}} = 2r_{\mathrm{SD}}I_{\mathrm{S}}^2 + \frac{\sqrt{2}U_{\mathrm{SD}}I_{\mathrm{S}}}{\pi}\left[2 - 2\cos\left(\frac{\beta}{2}\right)\right] \\ P_{\mathrm{s1}} = 2\sqrt{2}U_{\mathrm{in}}I_{\mathrm{p}}\sin\left(\frac{\alpha}{2}\right)\left(\frac{E_{\mathrm{on}}+E_{\mathrm{off}}}{U_{\mathrm{DD}}I_{D}} + \frac{Q_{\mathrm{RR}}}{I_{\mathrm{R\_D}}}\right)f_{\mathrm{s}} \\ P_{\mathrm{s2}} = 2\sqrt{2}U_{\mathrm{o}}I_{\mathrm{s}}\sin\left(\frac{\beta}{2}\right)\left(\frac{E_{\mathrm{on}}+E_{\mathrm{off}}}{U_{\mathrm{DD}}I_{\mathrm{D}}} + \frac{Q_{\mathrm{RR}}}{I_{\mathrm{R\_D}}}\right)f_{\mathrm{s}} \end{cases} \tag{13}$$

where P_{c1} and P_{s1} are the conduction loss and switching loss of the inverter, respectively, P_{c2} and P_{s2} are the conduction loss and switching loss of the rectifier, respectively, α and β are the phase shift angles of the inverter and rectifier, respectively, and U_{in} and U_{o} are the input and output voltage on the DC side. The remaining parameters are the inherent parameters of the converter.

For power semiconductor devices, the conduction resistance and conduction pressure drop are small compared with high-power multichannel IPT system, so the conduction loss can be neglected. Moreover, because the LCC-S compensation network is used in the high-power ISOP-IPT system, the inverters can achieve ZVS working state under the condition of full parameter resonance and effectively reduce the switching loss of the inverters. In addition, the full-bridge rectifier circuit usually adopts diode devices on the receiving side, and the switching loss is close to 0. Therefore, when analyzing the overall efficiency of the multichannel ISOP-IPT system, the loss caused by power converter is ignored to simplify the analysis process.

Figure 9 shows the steady-state circuit of each channel considering the resistance of the coils. $R_{\mathrm{p}i}$ and $R_{\mathrm{s}i}$ are the resistance of the transmitting coil and receiving coil of the coupler, respectively. The coil loss of each channel meets the following equation:

$$P_{i\_\mathrm{coil}} = I_{\mathrm{p}i}^2 R_{\mathrm{p}i} + I_{\mathrm{s}i}^2 R_{\mathrm{s}i} \tag{14}$$

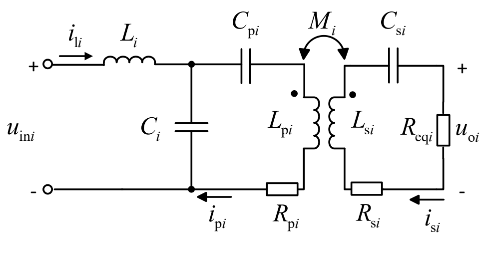

Figure 9. Steady-state circuit diagram of LCC-S compensation network considering coil resistance.

Under the resonant condition, the equation of receiver side circuit is:

$$j\omega M_i I_{\mathrm{p}i} = \left(R_{\mathrm{s}i} + R_{\mathrm{eq}i}\right) I_{\mathrm{s}i} \tag{15}$$

According to the above equation, the relationship between $I_{\mathrm{p}i}$ and $I_{\mathrm{s}i}$ is:

$$I_{\mathrm{p}i} = \frac{R_{\mathrm{s}i} + R_{\mathrm{eq}i}}{\omega M_i} I_{\mathrm{s}i} \tag{16}$$

By combining Equations (14) and (16), the overall coil loss equation of the ISOP-IPT system can be obtained:

$$P_{\text{coil}} = \sum_{i=1}^{n} I_{\text{s}i}^2 \left[\left(\frac{R_{\text{s}i} + R_{\text{eq}i}}{\omega M_i} \right)^2 R_{\text{p}i} + R_{\text{s}i} \right] \tag{17}$$

Based on the above analysis, the energy transfer efficiency equation of the multichannel ISOP-IPT system can be obtained:

$$\eta = \frac{P_{\text{out}}}{P_{\text{out}} + P_{\text{coil}}} = \frac{\sum\limits_{i=1}^{n} \frac{U_{\text{o}i}^2}{R_{\text{eq}i}}}{\sum\limits_{i=1}^{n} \frac{U_{\text{o}i}^2}{R_{\text{eq}i}} + P_{\text{coil}}} \tag{18}$$

Because the ISOP-IPT system adopts the parallel output structure, the output voltage of each channel is the same, and the equivalent impedance relationship of each channel is:

$$\sum_{i=1}^{n} \frac{1}{R_{\text{L}i}} = \frac{1}{R_{\text{L}}} \tag{19}$$

When the parameters of each channel in the system are consistent, Equations (6) and (19) can be substituted into Equation (18) to obtain:

$$\eta = \frac{1}{1 + \frac{8R_L}{\pi^2} \sum\limits_{i=1}^{n} \frac{1}{R_{\text{eq}i}^2} \left[\left(\frac{R_{\text{s}i} + R_{\text{eq}i}}{\omega M_i} \right)^2 R_{\text{p}i} + R_{\text{s}i} \right]} \tag{20}$$

Assuming that the resistance of the coupling coils of each channel is 0.2 Ω, the parameters of the compensation network are shown in Table 1. At this stage, the variation curve of the transmission efficiency for different number of channels is shown in Figure 10.

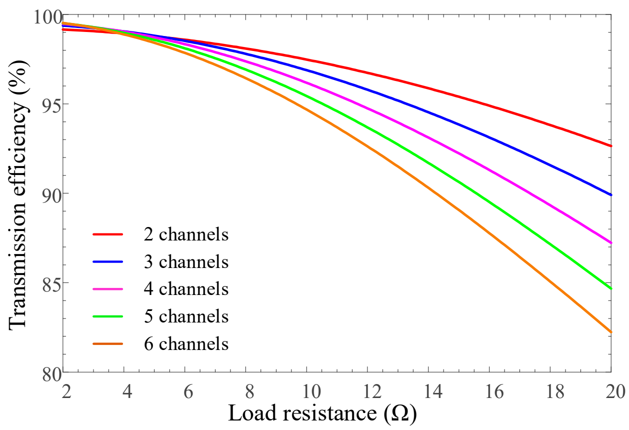

Figure 10. Efficiency curve of a multichannel ISOP-IPT system when the number of channels changes.

As can be seen from Figure 10, the ISOP-IPT system with LCC-S compensation network has CV output characteristics, so when the load impedance increases, the system transmission power decreases. When considering the coil loss, the transmission efficiency also decreases significantly with the decrease in the system transmission power, and the efficiency decline rate increases with the increase in the channel numbers and the load impedance. In the case of high power, the multichannel ISOP-IPT system has higher theoretical transmission efficiency, which is suitable for high-power application scenarios with high-voltage input and low-voltage output.

Based on Equation (20), the influence of imbalanced input voltage on transmission efficiency is analyzed. For the multichannel IPT system, the input voltage imbalance under resonant conditions is mainly caused by two factors: one is mutual inductance inconsistency, and the other is compensation parameter inconsistency. Based on the simulation model of the two-channel ISOP-IPT system, the influence of these two factors of voltage imbalance on the transmission efficiency of the system is analyzed. Parameters of the simulation model are shown in Table 1, and the resistance of each coil is 0.2 Ω. The simulation results are shown in Figure 11.

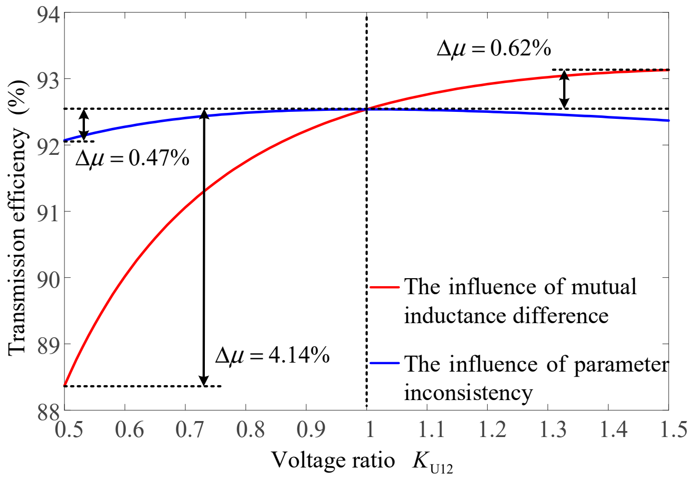

Figure 11. The influence curve of two voltage imbalance factors on the transmission efficiency of the ISOP-IPT system.

The blue curve in Figure 11 is the influence curve of system compensation parameter inconsistency on transmission efficiency. When the mutual inductance of the system remains unchanged and the compensation parameters satisfy the condition of full resonance, the change in the compensation parameters can be equivalent to the ratio change in the input voltage of the system. Then, combining Equations (2) and (20), it can be seen that the ratio of input voltage of each channel is inversely proportional to the ratio of equivalent load of each channel and the system transmission efficiency is affected by the equivalent load of each channel. Finally, with the increase in voltage imbalance caused by parameter inconsistency, the transmission efficiency of the system decreases.

Figure 11 shows the influence curve of mutual inductance inconsistency on system efficiency in red. When the system works in a resonant state, the mutual inductance of channel 1 is kept constant, and the mutual inductance of channel 2 is increased from 10 μH to 30 μH. At this time, the ratio of input voltage of each channel is proportional to the ratio of mutual inductance and satisfies Equation (2). When the mutual inductance of the two channels is equal, the input voltage can be equalized. The efficiency at $K_{U12} = 1$ is used as the standard. When K_{U12} is less than 1, the decrease in mutual inductance in channel 2 and the imbalanced input voltage will result in a decrease in system transmission efficiency. When K_{U12} is greater than 1, the mutual inductance of channel 2 increases, resulting in an increase in system efficiency. However, due to the voltage imbalance, the efficiency increase is inhibited. Therefore, the overall transmission efficiency of ISOP-IPT increases with the increase in mutual inductance of each channel.

In summary, the ISOP-IPT system can achieve higher transmission efficiency in high-power application scenarios with small load resistance. In addition, in order to improve the transmission efficiency of the system, the parameter design of each channel of the system should be designed according to the mutual inductance ratio so as to achieve input voltage equalization. On the basis of voltage equalization, it should be possible to increase the transmission mutual inductance of each channel.

4. Experiments and Discussions

4.1. Construction of Two-Channel ISOP-IPT System Experiment Platform

The experimental platform of the two-channel ISOP-IPT system was built to verify the correctness of the theoretical analysis. The experimental platform is shown in Figure 12. The digital signal processing (DSP) module containing a TMS320F28335 processor and field programmable gate array (FPGA) module for generating driving signals are used in the control part of the system. The inverter MOSFET model is C2M0025120D. The diode model of the rectifier is APT30SCD120. The power supply model is IT-6000-800C (ITECH, Nanjing, China), and the maximum power is 12 kW. The system operating frequency is 85 kHz. The coupling coil size is 650 mm × 650 mm, and the transmission distance is 10 cm. The compensation network parameters of the system are shown in Table 2.

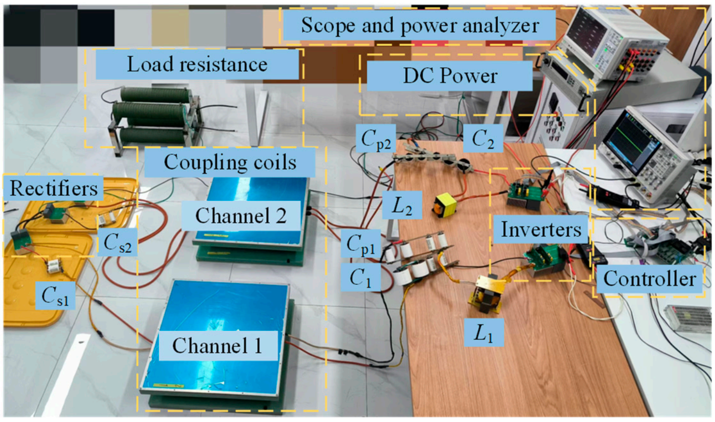

Figure 12. Experimental platform of 2-channel ISOP-IPT system.

Table 2. Experimental parameters of 2-channel ISOP-IPT system.

Symbol	Value	Symbol	Value
$L_1/\mu H$	23.94	C_1/nF	146.65
$L_2/\mu H$	24.12	C_2/nF	145.3
$L_{p1}/\mu H$	96.11	C_{p1}/nF	48.37
$L_{p2}/\mu H$	95.07	C_{p2}/nF	49.23
$L_{s1}/\mu H$	96.62	C_{s1}/nF	36.55
$L_{s2}/\mu H$	95.04	C_{s2}/nF	36.58
$M_1/\mu H$	22.3	$M_2/\mu H$	22.48
R_{p1}/Ω	0.2	R_{s1}/Ω	0.19
R_{p2}/Ω	0.17	R_{s2}/Ω	0.22
R_L/Ω	5~40	f/kHz	85
U_{in}/V	470		

4.2. Verification of Voltage Imbalance Effect of the System

(A) Working status of the inverter

In order to analyze the inverter output voltage and current variation in each channel when the system voltage is imbalanced, the mutual inductance of channel 2 is increased from 22.48 μH to 25.81 μH. At this time, the inverter output of each channel of the system is shown in Figure 13. It can be seen that due to the increase in mutual inductance in channel 2, the degree of imbalance in DC input voltage of the system increases. For the channel with low input voltage, the instantaneous value of the output current at the switching time of the inverter decreases. The correctness of the theoretical analysis in Section 3.1 is verified. If the mutual inductance and voltage imbalance of the system increase further, it will eventually cause a channel to lose the ZVS working state, which will reduce the stability of the overall multichannel ISOP-IPT system.

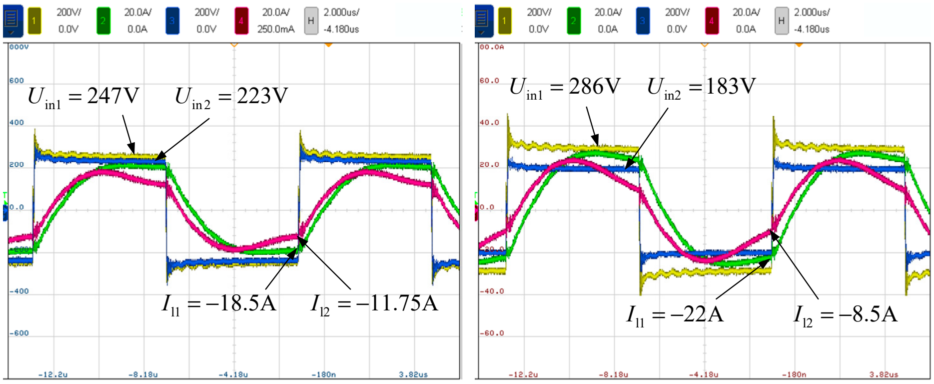

(a) M_2=22.48 µH (b) M_2=25.81 µH

Figure 13. Inverter output waveform diagram of each channel when mutual inductance changes.

(B) Transmission efficiency of the system

Firstly, the effect of load resistance change on the efficiency of the system is verified. Adjust the load resistance from 5 Ω to gradually increase to 40 Ω, and the efficiency change at this time is shown in Figure 14. Moreover, the system efficiency measurements at 5 Ω to 20 Ω are given in Figure 15. When the load resistance is 5 Ω, the system efficiency is low due to the weak heat dissipation capacity of the rectifier module and the high diode temperature. When the system load increases from 10 Ω to 40 Ω, the overall transmission efficiency of the system gradually decreases from the highest 94.03% to 89.38%. The experimental results show that the transmission efficiency of the two-channel ISOP-IPT system decreases with the decrease in power level, which verifies the correctness of the theoretical analysis.

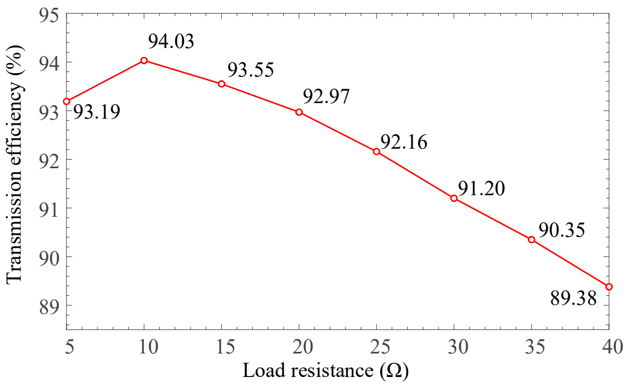

Figure 14. Change in transmission efficiency of 2-channel ISOP-IPT system when load resistance changes.

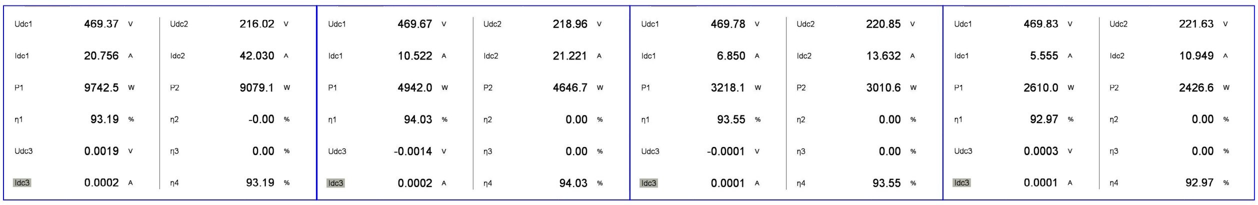

(a) 5 Ω (b) 10 Ω (c) 15 Ω (d) 20 Ω

Figure 15. System transmission efficiency at different loads.

Then, the effect of voltage imbalance caused by inconsistent network parameters on the transmission efficiency of multichannel system is proved. Based on the experimental platform built with the parameters shown in Table 2, the compensation network parameters of channel 2 were changed. The series compensation inductance of channel 2 is first reduced to 13.57 µH and then increased to 35.95 µH. The other compensation network elements are configured according to the resonant condition. The compensation network parameters after the change in channel 2 are shown in Table 3, and the load resistance is 10 Ω.

Table 3. Compensation network parameters of corresponding channel after inductance change.

Symbol	Value	Symbol	Value
$L'_2/\mu H$	13.57	C'_2/nF	258.5
C'_{p2}/nF	43.2	C'_{s2}/nF	36.58
$L''_2/\mu H$	35.95	C''_2/nF	97.38
C''_{p2}/nF	58.9	C''_{s2}/nF	36.6

Figure 16 shows the DC input voltage and transmission efficiency of the system when the series compensation inductance on the transmitting side of channel 2 is reduced. At this time, the total input voltage of the system is 470 V, so 235 V is taken as the target value when the input voltage of each channel is equalized. It can be seen that when the series compensation inductance of the transmitting side of channel 2 decreases, the DC input voltage of the corresponding channel also decreases. At this time, the system voltage imbalance degree before the compensation parameter changes in Figure 13a is 5.11%. In Figure 16, the voltage imbalance degree after the compensation parameter changes is 25.74%. In Figure 15b, the transmission efficiency of the system before the compensation parameter changes is 94.03%. In Figure 16, the transmission efficiency of the system after compensation parameter changes is 93.32%.

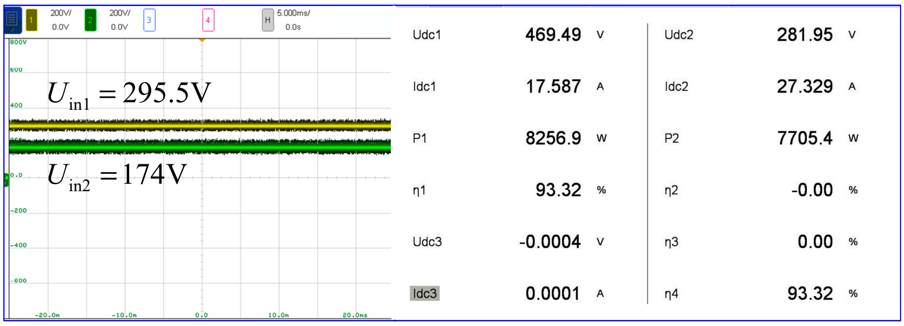

Figure 16. System input voltage and transmission efficiency when channel 2 series compensating inductance L'_2 = 13.57 μH.

Figure 17 shows the DC input voltage and transmission efficiency of the system when the series compensation inductance on the transmitting side of channel 2 is increased. It can be seen that when the series compensation inductance of the transmitting side of channel 2 increases, the DC input voltage of the corresponding channel also increases. At this time, the voltage imbalance degree of the system increases from 5.11% to 22.34%, and the transmission efficiency decreases from 94.03% to 93.79%.

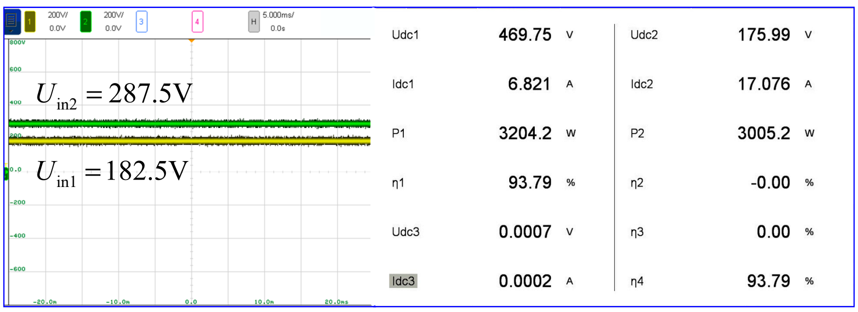

Figure 17. System input voltage and transmission efficiency when channel 2 series compensating inductance L''_2 = 35.95 μH.

To sum up, when the parameters of the compensation network of the system change, the degree of input voltage imbalance increases, and the proportion of change satisfies Equation (2). Compared with the 94.03% transmission efficiency when the system input voltage is equalized, the transmission efficiency decreases by 0.71% and 0.24% respectively when the parameters of the compensation network change. It is proved that the input voltage imbalance caused by the change in compensation network parameters will lead to the decrease in system transmission efficiency.

Finally, the effect of voltage imbalance caused by mutual inductance inconsistency on the transmission efficiency of multichannel system is proved. Since the compensation network parameters of each channel in Table 2 are basically the same, the parameters in Table 2 are used as standard parameters. The transmission mutual inductance of channel 2 is gradually increased from 19.3 μH, and the change in transmission efficiency of the system at this time is shown in Figure 18. It can be seen that the overall transmission efficiency of the system increases with the increase in mutual inductance in channel 2. When the mutual inductance of channel 2 deviates from the standard value, it can be seen from Equation (2) that the imbalance degree of DC input voltage of the system increases. When the mutual inductance of channel 2 is less than the standard value, the effect of mutual inductance and voltage imbalance is superimposed on each other, and the system efficiency decreases more. When the mutual inductance of channel 2 is greater than the standard value, the effects of mutual inductance and voltage imbalance cancel each other, and the system efficiency is less improved. The overall experimental results are basically consistent with the trend of simulation results, which verifies the correctness of the theoretical analysis in Section 3.2.

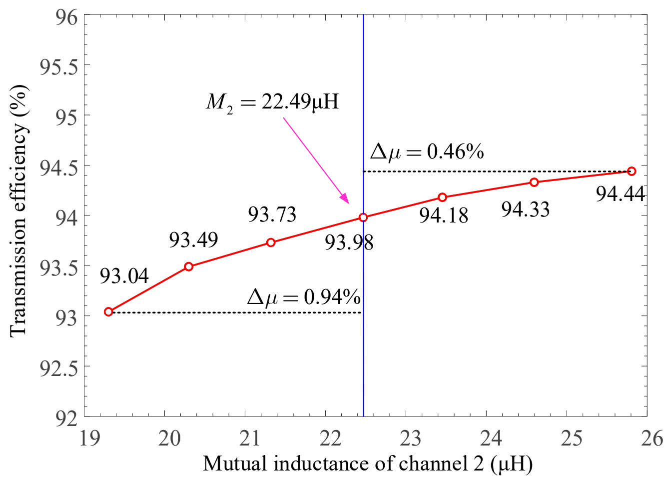

Figure 18. Change in system transmission efficiency when mutual inductance of channel 2 changes.

5. Conclusions

In this paper, a multichannel ISOP-IPT system suitable for low-voltage high-power output is analyzed for the application scenario of EV fast charging, and the following conclusions are drawn. Firstly, in the ISOP-IPT system based on the LCC-S compensation network, the parameter deviation of the compensation capacitor in parallel on the transmitting side and the compensation capacitor in series on the receiving side will cause input voltage imbalance. In addition, when each channel meets the resonant condition, the change in compensation parameters and mutual inductance will also lead to voltage imbalance. The voltage imbalance will reduce the stability of the system and affect the energy transmission efficiency. When the resistance of the coupler coil is considered, the transmission efficiency of the system decreases with the increase in load and increases with the increase in mutual inductance. This is why the circuit structure analyzed in this paper is suitable for low-voltage and high-power scenarios. In the parameter design of the system, it is necessary to ensure that the input voltage of each channel is equal and the mutual inductance of each channel is increased as much as possible so as to improve the energy transmission efficiency of the system. Finally, a two-channel experimental platform was built to verify the correctness of the theoretical analysis on the influence of transmission efficiency, and the maximum system efficiency was 94.03%.

How to solve the problem of imbalanced input voltage of a multichannel ISOP-IPT system and realize the output control of the system can become an important research direction in the future. Corresponding system control methods can be proposed to achieve transmission power distribution and improve the operating stability of multichannel systems. In addition, the influence of rectifier temperature on system transmission efficiency and the design of corresponding heat dissipation structure can also be a suitable avenue of research.

Author Contributions: Conceptualization, L.W. and P.S.; methodology, L.W. and Y.L.; validation, L.W. and Y.L.; writing—original draft preparation, L.W.; writing—review and editing, P.S., Y.L., X.W. and E.R.; funding acquisition, P.S. and X.W. All authors have read and agreed to the published version of the manuscript.

Funding: This research was funded by the National Key Research and Development Program of China, grant 2022YFC3102800, and the National Natural Science Foundation of China, grants 52007195 and 52207182.

Data Availability Statement: Data are contained within the article.

Conflicts of Interest: The authors declare no conflicts of interest.

References

1. Xie, R.; Liu, R.; Chen, X.; Mao, X.; Li, X.; Zhang, Y. An Interoperable Wireless Power Transmitter for Unipolar and Bipolar Receiving Coils Based on Three-Switch Dual-Output Inverter. *IEEE Trans. Power Electron.* **2024**, *39*, 1985–1989. [CrossRef]
2. Zhou, W.; Chen, Z.; Zhang, Q.; Li, Z.; Huang, L.; Mai, R.; He, Z. Design and Analysis of CPT System with Wide-Range ZVS and Constant Current Charging Operation Using 6.78 MHz Class-E Power Amplifier. *IEEE J. Emerg. Sel. Top. Power Electron.* **2024**, *in press*. [CrossRef]
3. Aydin, E.; Aydemir, M.T.; Aksoz, A.; El Baghdadi, M.; Hegazy, O. Inductive Power Transfer for Electric Vehicle Charging Applications: A Comprehensive Review. *Energies* **2022**, *15*, 4962. [CrossRef]
4. Zhou, W.; Tang, D.; Chen, Z.; Mai, R.; He, Z. Nonisolation Model and Load Virtual-Grounding Design Method for Capacitive Power Transfer System with Asymmetric Four-Plate Coupling Interface. *IEEE J. Emerg. Sel. Top. Power Electron.* **2024**, *12*, 208–218. [CrossRef]
5. Nithiyanandam, V.; Sampath, V. Approach-Based Analysis on Wireless Power Transmission for Bio-Implantable Devices. *Appl. Sci.* **2023**, *13*, 415. [CrossRef]
6. Wen, H.; Li, J.; Zhang, K.; Ye, J.; Yan, Z.; Song, B.; Tong, X. Enhancing Power Transmission Stability of AUV's Wireless Power Transfer System with Compact Planar Magnetic Coupler. *J. Mar. Sci. Eng.* **2023**, *11*, 566. [CrossRef]
7. Rong, E.; Sun, P.; Qiao, K.; Zhang, X.; Yang, G.; Wu, X. Six-Plate and Hybrid-Dielectric Capacitive Coupler for Underwater Wireless Power Transfer. *IEEE Trans. Power Electron.* **2024**, *39*, 2867–2881. [CrossRef]
8. Laha, A.; Kalathy, A.; Pahlevani, M.; Jain, P. A Comprehensive Review on Wireless Power Transfer Systems for Charging Portable Electronics. *Eng.* **2023**, *4*, 1023–1057. [CrossRef]
9. Wu, S.; Cai, C.; Zhang, H.; Liu, X.; Chai, W. A Free-Positioning IPT System via Reconfigurable Coil Array Transmitter for Unmanned Aerial Vehicle Applications. *IEEE Trans. Transp. Electrif.* 2024; *in press*. [CrossRef]
10. Liu, X.; Gao, F.; Zhang, Y.; Khan, M.M.; Zhang, Y.; Wang, T.; Rogers, D.J. A Multi-Inverter High-power Wireless Power Transfer System with Wide ZVS Operation Range. *IEEE Trans. Power Electron.* **2022**, *37*, 14082–14095. [CrossRef]
11. Yuan, H.; Wang, C.; Xia, D. Research on Input-Parallel Single-Switch WPT System with Load−Independent Constant Voltage Output. *IEEE Trans. Transp. Electrif.* **2023**, *9*, 1888–1896. [CrossRef]
12. Liu, X.; Gao, F.; Wang, T.; Khan, M.M.; Zhang, Y.; Xia, Y.; Wheeler, P. A Multi-Inverter Multi-rectifier Wireless Power Transfer System for Charging Stations with Power Loss Optimized Control. *IEEE Trans. Power Electron.* **2023**, *38*, 9261–9277. [CrossRef]
13. Deng, Q.; Wang, L.; Luo, P.; Czarkowski, D.; Hu, W. Multi-channel inductive power transfer system based on ISOP topology. *J. Power Electron.* **2024**, *24*, 503–514. [CrossRef]
14. Qu, X.; Yao, Y.; Wang, D.; Wong, S.-C.; Tse, C.K. A family of hybrid IPT topologies with near load-independent output and high tolerance to pad misalignment. *IEEE Trans. Power Electron.* **2019**, *35*, 6867–6877. [CrossRef]
15. Bagchi, A.C.; Kamineni, A.; Zane, R.A.; Carlson, R. Review and Comparative Analysis of Topologies and Control Methods in Dynamic Wireless Charging of Electric Vehicles. *IEEE J. Emerg. Sel. Top. Power Electron.* **2021**, *9*, 4947–4962. [CrossRef]
16. Tran, M.T.; Thekkan, S.; Polat, H.; Tran, D.-D.; El Baghdadi, M.; Hegazy, O. Inductive Wireless Power Transfer Systems for Low-voltage and High-Current Electric Mobility Applications: Review and Design Example. *Energies* **2023**, *16*, 2953. [CrossRef]
17. Yang, J.; Liu, R.; Tong, Q.; Yang, X.; Liu, Q.; Yao, A. Multi-Objective Optimization of LCC-S-Compensated IPT System for Improving Misalignment Tolerance. *Appl. Sci.* **2023**, *13*, 3666. [CrossRef]

18. Zhang, X.; Cai, T.; Duan, S.; Feng, H.; Hu, H.; Niu, J. A Harmonic-considered Time Domain Model of LCC Compensated Wireless Power Transfer Systems. In Proceedings of the 2018 IEEE International Power Electronics and Application Conference and Exposition (PEAC), Shenzhen, China, 4–7 November 2018; pp. 1–5. [CrossRef]
19. Hu, H.; Cai, T.; Duan, S.; Zhang, X.; Niu, J.; Feng, H. An Optimal Variable Frequency Phase Shift Control Strategy for ZVS Operation Within Wide Power Range in IPT Systems. *IEEE Trans. Power Electron.* **2020**, *35*, 5517–5530. [CrossRef]
20. Liu, S.; Mai, R.; Zhou, L.; Li, Y.; Hu, J.; He, Z.; Yan, Z.; Wang, S. Dynamic Improvement of Inductive Power Transfer Systems with Maximum Energy Efficiency Tracking Using Model Predictive Control: Analysis and Experimental Verification. *IEEE Trans. Power Electron.* **2020**, *35*, 12752–12764. [CrossRef]